Strojniški vestnik - Journal of Mechanical Engineering 55(2009)7-8, 484-493
UDC 629.7

Paper received: 05.03.2009
Paper accepted: 08.07.2009

Model-Based Investigation of Flight Qualities: the Theory and Practice of Full-Scale Aircraft Modelling

Tine Tomažič[1,*] - Drago Matko[2]
[1] Pipistrel d.o.o. Ajdovščina, Advanced Light Aircraft, Slovenia
[2] University of Ljubljana, Faculty of Electrical Engineering, Slovenia

The paper presents combined modelling of a full-scale aircraft. Here theoretical model of the real motorglider is developed and linearised, while the parameters are estimated also through identification of measured data. The transfer functions for roll and pitch behaviour obtained theoretically and experimentally are compared and validated. The obtained models match real vehicle behaviour satisfactorily, thus enabling designers to test-fly the aircraft in a virtual environment already during the development phase with a large degree of certainty. This results in significant time and cost savings and may also avoid expensive prototype modifications that are otherwise often necessary.

Keywords: aeroplanes, modelling, flying, properties

0 INTRODUCTION

The aim of the research was to validate a purely-theoretical aircraft model by comparing the results with the actual in-flight measurements on a full-scale vehicle. Despite having developed and used the theoretical model successfully for simulator-based hardware-in-the-loop autopilot tuning for Unmanned Aerial Vehicles (UAVs) [1] it was not clear how well this approach would describe the behaviour of a real, full scale aircraft. It should be noted that the chosen theoretical model development methodology does not take into account the coupling of adjacent fixed and moving aerodynamic structures (e.g. wing-aileron aerodynamic coupling) but regards the structures as a purely individual object moving through air instead. With small-sized aircraft (UAVs) the difference in simulated and actual behaviour due to the above mentioned model simplification is hardly noticeable and can be regarded as insignificant, but the implications of such an approach on full-scale aircraft remained unknown before the validation was carried out.

Very few attempts of identification of dynamic properties for light aircraft exist [2] and none of them attempted to use modelling and identification techniques to support initial development of the light aircraft.

The aircraft chosen for the theoretical model validation was the Pipistrel Sinus 912 motorglider (Fig. 1, Table 1). As motorgliders have longer wings and ailerons [3] than conventional aircraft, the effect of aerodynamic coupling between these structures is emphasized more. As a direct result the differences between the anticipated theoretical model and real responses are expected to be greater.

The approach used in this paper was to assemble a PQ (angular velocities around two aircraft's axis in coordinate system of the aircraft) model based on system identification of actual flight data.

Then, simulated outputs of both, the theoretical and identified aircraft PRQ models, using various inputs were compared and evaluated.

Fig. 1. *Pipistrel Sinus 912 used for model validation*

*Corr. Author's Address: Pipistrel d.o.o. Ajdovščina, Goriška cesta 50a, SI-5270 Ajdovščina, Slovenia, tine@pipistrel.si

Table 1. *Pipistrel 912 basic data*

Proportions	
Wing span	14.97 m
Length	6.60 m
Height	1.70 m
Wing area	12.26 m^2
Horizontal tail area	1.63 m^2
Vertical tail area	1.10 m^2
Aspect ratio	18.3
Weights	
Empty weight	285 kg
Modelling set-point	420 kg
Performance	
Minimum speed	63 km/h
Maximum speed	225 km/h
Modelling set-point	140 km/h
Glide ratio (engine off)	1:27

As the validation of the theoretical model [4] uses only the acquired flight data, all work was focused around a single, linear dynamic PQ aircraft model. The set point, defined with airspeed and aircraft's weight is set at mid-range taking into account the operational envelope of the aircraft. This set point not only provides the most general approximation of the aircraft's behaviour, but also matches the aircraft's manoeuvring speed and weight. Around the chosen set point, the aircraft is most manoeuvrable and full deflections of flight controls can be used without causing damage to the airframe and crew.

The paper is organised as follows: in Chapter 2 the theoretical model of the aircraft is given. The well known 12 degree of freedom state space model is used for linearization and for developing two simple second order transfer functions (aileron to roll and elevator to pitch). In Chapter 3 the real measured data are used for parameter estimation of the abovementioned transfer functions and the resulting model is compared with the theoretical one. Both models are also validated using measured data. In the conclusion some comments of the proposed models usability are given.

1 THEORETICAL AIRCRAFT MODEL

The well known 12 degree of freedom [4] model is used. The outputs of the model are the same as its states and are comprised in the vector:

$$x = \begin{bmatrix} u & v & w & P & Q & R & \Phi & \Theta & \Psi & X_E & Y_E & Z_E \end{bmatrix}$$

where the symbols in order of appearance mean: velocities in x, y and z coordinates, roll rate, pitch rate, yaw rate (all these in aircraft co-ordinate system: x into the direction of nose, y to the right wing, z down), yaw angle, pitch angle, roll angle, X, Y and Z coordinates in the Earth's coordinate system.

There are also 8 inputs considered, namely left aileron deflection (δ_{ailL}), right aileron deflection (δ_{ailR}), left elevator deflection (δ_{elevL}), right elevator deflection (δ_{elevR}), rudder deflection (δ_{rud}), flaps extension (δ_{flaps}), speed-brakes extension (δ_{spdbrk}) and the centerline engine force (F_{Thrust}). The set of motion equations, most suitable for aircraft dynamic simulations is as follows:

$$\dot{u} = \frac{F_{XAero}}{m} - g\sin\Theta - Qw + Rv + \frac{F_{Thrust}}{m} \tag{2.1}$$

$$\dot{v} = \frac{F_{YAero}}{m} - g\cos\Theta\sin\Phi - Ru + Pw \tag{2.2}$$

$$\dot{w} = \frac{F_{ZAero}}{m} - g\cos\Theta\cos\Phi - Pv + Qu \tag{2.3}$$

$$\dot{P} = \frac{L + QRI_y - QRI_z}{I_x} \tag{2.4}$$

$$\dot{Q} = \frac{M + PRI_z - PRI_x}{I_y} \tag{2.5}$$

$$\dot{R} = \frac{N + PQI_x - PQI_y}{I_z} \tag{2.6}$$

$$\dot{\Phi} = P + Q\sin\Phi\tan\Theta + R\cos\Phi\tan\Theta \tag{2.7}$$

$$\dot{\Theta} = Q\cos\Phi + R\sin\Phi \tag{2.8}$$

$$\dot{\Psi} = \frac{Q\sin\Phi + R\cos\Phi}{\cos\Theta} \tag{2.9}$$

$$\begin{aligned}\dot{X}_E &= u(\cos\Theta\cos\Psi) + v(\sin\Phi\sin\Theta\cos\Psi) + \\ &+ w(\cos\Phi\sin\Theta\cos\Psi + \sin\Phi\sin\Psi)\end{aligned} \tag{2.10}$$

$$\begin{aligned}\dot{Y}_E &= u(\cos\Theta\sin\Psi) + v(\sin\Phi\sin\Theta\sin\Psi) + \\ &+ w(\cos\Phi\sin\Theta\sin\Psi + \sin\Phi\cos\Psi)\end{aligned} \tag{2.11}$$

$$\dot{Z}_E = u(\sin\Theta) + v(\sin\Phi\cos\Theta) + w(\cos\Phi\cos\Theta)\,. \tag{2.12}$$

Equations (2.1) to (2.3) describe translations (speed) and can be transformed to the airspeed (V), angle of attack (α) and sideslip angle (β) set by vector rules:

$$V = \sqrt{u^2 + v^2 + w^2} \tag{2.13}$$

$$\alpha = \arctan \frac{w}{u} \tag{2.14}$$

$$\beta = \arcsin \frac{v}{\sqrt{u^2 + w^2}} \ . \tag{2.15}$$

Equations (2.4) to (2.6) describe angular velocities: roll rate (*P*), pitch rate (*Q*) and yaw rate (*R*) for the aircraft. All are expressed in the x,y,z coordinate system of the aircraft (local coordinate system).

Equations (2.7) to (2.9) are Euler angles, hence angles of roll (Φ), pitch (Θ) and yaw (Ψ) in which the aircraft appears to the viewer. All are in the Earth's X ,Y, Z coordinate system (global coordinate system). Equations (2.10) to (2.12) describe the aircraft's relative position to the centre of the Earth's coordinate system.

L, M and *N* in Egs. (2.4) to (2.6) are moments around the x, y and z body axis of the airplane. Other parameters in Eqs. (2.1) to (2.12) are: *m* – mass of the aircraft, *g* – gravity constant and I_x, I_y and I_z – the moments of inertia around the x,y and z body axis of the airplane.

The sum of forces *F*, which act on the aircraft being the body in motion, can be regarded as the sum of aerodynamic, gravity and engine (thrust) forces as follows:

$$F_x = F_{XAero} - mg\sin\Theta + F_{Thrust} \tag{2.16}$$

$$F_y = F_{YAero} + mg\cos\Theta\sin\Phi \tag{2.17}$$

$$F_z = F_{ZAero} + mg\cos\Theta\cos\Phi \tag{2.18}$$

1.1 Modelling of Aerodynamic Properties

This section provides an insight on how aircraft's aerodynamic properties are modelled. The basic aim is to determine aerodynamic forces and moments labelled F_{XAero}, F_{YAero}, F_{ZAero} and *L, M* and *N*. Normally wing-tunnel data are used to determine an aircraft's aerodynamic properties. However, using 2D data for airfoil shapes and fuselage drag can also lead to adequate results.

This is also the approach used in the theoretical aircraft model development presented in this paper.

Before any further formulae are given the reader must be aware of certain terms and assumptions. Most aerodynamic equations linking shape properties, the speed of travelling through the air and forces/moments include α (angle of attack of structure moving through a medium, Eq. (2.14), β (sideslip angle, Eq. (2.15), *q* (dynamic pressure or local airspeed) and a certain kind of coefficient (*C* – describing non-linearities among variables). To simplify the formulae the following non-critical assumption is often made: α of the wing itself equals α of the rest of aircraft's body.

The basic equations describing forces of aerodynamic lift and drag are:

$$F_L = q \cdot S \cdot C_L \tag{2.19}$$

$$F_D = q \cdot S \cdot C_D \, , \tag{2.20}$$

where C_L and C_D are coefficients of lift and drag, *S* is the reference cross-section of body moving through the air, in this case the wing, and *q* is dynamic pressure defined as:

$$q = \frac{\rho \cdot V^2}{2} \tag{2.21}$$

where ρ is density of air and *V* is the total velocity defined as in Eq. (2.13). In practice, *V* is the true airspeed already corrected for angle of attack α and sideslip β. For normal flight circumstances, that is around the chosen set point, which is in the middle of aircraft's speed and angle of attack envelope, it is assumed that C_L is approximately linearly dependant on angle of attack α. Hence:

$$F_L = q \cdot S \cdot C_{L\alpha} \cdot \alpha \tag{2.22}$$

for side-lift, which is linked to sideslip angle β, the relation is similar. Note that most non-linearities are accounted for in $C_{L\alpha}$.

One has to be aware of the fact that the centre of aerodynamic forces does not correspond to the centre of gravity of the aircraft. As the aerodynamic forces grab dislocated from the centre of gravity, they also cause moments. A complete set of generalised aerodynamic forces and moments are presented in Eqs. (2.23) to (2.28).

The index B stands for "Body" as these are forces and moments that act on the aircraft in the situation where the controls are in neutral position and not deflected. As the lift and drag are defined as forces being perpendicular and parallel to the plane of wings respectively, one must respect the angle of attack in *Fx* and *Fz* expressions:

$$F_{XB} = F_L \sin\alpha - F_D \cos\alpha \tag{2.23}$$

$$F_{YB} = q \cdot S \cdot C_{Y\beta} \cdot \beta \tag{2.24}$$

$$F_{ZB} = -F_L \cos\alpha - F_D \sin\alpha \quad (2.25)$$

$$L_B = q \cdot S \cdot l \cdot C_{L\beta} \cdot \beta \quad (2.26)$$

$$M_B = q \cdot S \cdot l \cdot C_{M\alpha} \cdot \alpha \quad (2.27)$$

$$N_B = q \cdot S \cdot l \cdot C_{N\beta} \cdot \beta \quad (2.28)$$

In Eqs. (2.26) through (2.28) l is the reference distance between the centre of gravity and the centre of aerodynamic forces, which is in most cases also dependent on airspeed.

We have covered aerodynamic properties of the aircraft's body itself so far. Next are the effects of control surfaces. Normally there are three main control surfaces on the aircraft, namely the ailerons, elevator and the rudder. Their primary functions are to control roll-, pitch- and yaw-rates respectively. They of course also cause forces and moments with their applications (deflections marked as δ_i):

$$F_{YC} = q \cdot S \cdot C_{L\delta} \cdot \delta_{rud} \quad (2.29)$$

$$F_{ZC} = q \cdot S \cdot C_{L\delta} \cdot \delta_e \quad (2.30)$$

$$L_C = 2 \cdot q \cdot S \cdot C_{L\delta} \cdot \delta_a \cdot l_{CS} \quad (2.31)$$

$$M_C = F_{ZC} \cdot l_{CS} \quad (2.32)$$

$$N_C = F_{YC} \cdot l_{CS} \ . \quad (2.33)$$

The index C stands for control surfaces, l_{CS} is the distance between the discussed control surface and the centre of gravity of the aircraft. While some aircraft use amount different deflections in left and right aileron/elevator, this can be in most cases simplified to using a single control surface respectively, i.e. δ_a (combined aileron effect) *and* δ_e (combined elevator effect) above.

The complete set of aerodynamic forces and moments are obtained by joining forces and moments caused by body and control surfaces aerodynamics:

$$F_{XAero} = F_{XB} \quad (2.34)$$

$$F_{YAero} = F_{YB} + F_{YC} \quad (2.35)$$

$$F_{ZAero} = F_{ZB} + F_{ZC} \quad (2.36)$$

$$L = L_B + L_C \quad (2.37)$$

$$M = M_B + M_C \quad (2.38)$$

$$N = N_B + N_C \ . \quad (2.39)$$

1.2 Linearisation of the Model

In this section a simplified second order linear model for pitch and roll behaviour will be analytically calculated from the non-linear theoretical model, later serving as a basis for comparison with the identified models.

With regard to the Subsection 2.1 it can be observed that the theoretical model is obtained by a series of calculations. First, forces and moments which arise from the aircraft's flight, aerodynamics linked to control deflections and outside influences e.g. wind and turbulence must be determined. These forces and moments further serve to compute the equations of motion, which are described by (2.1) to (2.12). As the objective of this paper is to compare the theoretical PQ aircraft model against its identified counterpart, the set of 12 equations of motion can be reduced to 6 equations, all defined in the coordinate system of the aircraft. With PQ modelling the focus is on aircraft's dynamic behaviour, but not on its position in the global earth coordinate system.

Eqs. (2.1) to (2.6) are further reduced to obtain the pitch-behaviour and roll-behaviour model.

The assumptions for the pitch-behaviour model are as follows: there is no sideways movement, hence v (component of airspeed V along the y axis) is 0, thereby also P and R are 0, α is small, θ is small and Φ is zero.

The nonlinear pitch-behaviour is described with:

$$\dot{u} = \frac{F_{XAero}}{m} - g\sin\Theta - Qw + \frac{F_{Thrust}}{m} \quad (2.40)$$

$$\dot{w} = \frac{F_{ZAero}}{m} - g\cos\Theta + Qu \quad (2.41)$$

$$\dot{Q} = \frac{M}{I_y},\ \dot{\Theta} = Q \ . \quad (2.42)$$

The nonlinear roll-behaviour model where u (component of airspeed V along the x axis) is 0, and consequentially also Q and R are 0, β is small, Φ is small and θ is zero, is given in the following form:

$$\dot{v} = \frac{F_{YAero}}{m} - g\sin\Phi + Pw \quad (2.43)$$

$$\dot{w} = \frac{F_{ZAero}}{m} - g\cos\Phi - Pv \quad (2.44)$$

$$\dot{P}=\frac{L}{I_x},\ \dot{\Phi}=P\ . \tag{2.45}$$

1.3 Pitch Linear Model

As we are focusing on pitch-behaviour i.e. the pitch rate Q, the expressions (2.40) and the second part of (2.42) can be omitted. Expression (2.40) indeed contains the pitch rate Q in its relation, however it describes only the forward motion of the aircraft and is decoupled from Eqs. (2.41) and (2.42). Before writing the linearised model from which the transfer function with δ_e as the input and Q as the output is derived, we must take into account that all lift, drag, gravity and propulsion forces cancel each-other in the chosen set-point (level unaccelerated flight conditions). The corresponding linear form is finally obtained:

$$\dot{w}=\frac{-F_L+F_{ZC}}{m},\ \dot{Q}=\frac{M}{I_y}\ . \tag{2.46}$$

After a little algebra the following form, with derivatives of Q on the left side of the equation and the derivatives of δ_e on the right side is derived:

$$\begin{aligned}
&s^2Q+sQ\left(\frac{q\cdot S_{wing}\cdot C_{L\alpha}}{u_0\cdot m}-\frac{q\cdot S_{wing}\cdot C_{M\alpha}\cdot l_{cp}\cdot l}{I_y}\right)+\\
&+Q\left(\frac{q^2\cdot S_{wing}^2\cdot C_{L\alpha}\cdot C_{M\alpha}\cdot l_{cp}\cdot l}{u_0\cdot I_y\cdot m}-\frac{q\cdot S_{wing}\cdot C_{M\alpha}\cdot l_{cp}\cdot l_{cs}}{u_0\cdot I_y\cdot m}\right)=\\
&=s\delta_e\left(\frac{q\cdot S_{elev}\cdot C_{L\delta}\cdot l_{cs}}{I_y}\right)+\\
&+\delta_e\left(\frac{q^2\cdot S_{wing}\cdot S_{elev}\cdot C_{M\alpha}\cdot C_{L\delta}}{u_0\cdot I_y\cdot m}-\frac{q^2\cdot S_{wing}\cdot S_{elev}\cdot C_{L\alpha}\cdot C_{L\delta}\cdot l_{cs}}{u_0\cdot I_y\cdot m}\right)
\end{aligned} \tag{2.47}$$

Note that l_{cp} is the distance from the centre of propulsion forces (thrust) to control surface and comes from the damping effect.

The corresponding transfer function is:

$$\frac{Q(s)}{\delta_e(s)}=\frac{b_1s+b_0}{s^2+a_1s+a_0}\ , \tag{2.48}$$

where δ_e is the combined deflection effect of the elevator in radians (positive is down). Coefficients a_i and b_i in Eq. (2.48) are as follows:

$$a_1=\frac{q\cdot S_{wing}\cdot C_{L\alpha}}{u_0\cdot m}-\frac{q\cdot S_{wing}\cdot C_{M\alpha}\cdot l_{cp}\cdot l}{I_y}$$

$$a_0=\frac{q^2\cdot S_{wing}^2\cdot C_{L\alpha}\cdot C_{M\alpha}\cdot l_{cp}\cdot l}{u_0\cdot I_y\cdot m}-\frac{q\cdot S_{wing}\cdot C_{M\alpha}\cdot l_{cp}\cdot l_{cs}}{u_0\cdot I_y\cdot m}$$

$$b_1=\frac{q\cdot S_{elev}\cdot C_{L\delta}\cdot l_{cs}}{I_y}$$

$$b_0=\frac{q^2\cdot S_{wing}\cdot S_{elev}\cdot C_{M\alpha}\cdot C_{L\delta}}{u_0\cdot I_y\cdot m}-\frac{q^2\cdot S_{wing}\cdot S_{elev}\cdot C_{L\alpha}\cdot C_{L\delta}\cdot l_{cs}}{u_0\cdot I_y\cdot m}$$

In case of Sinus 912 motorglider and the set point described in Subsection 2.2 the Eq. (2.48) becomes:

$$\frac{Q(s)}{\delta_e(s)}=\frac{6.6600s+1.9280}{s^2+0.3733s+0.1650} \tag{2.49}$$

1.4 Roll Linear Model

Here similar approach as in Subsection 2.3 is used. For roll, we are most interested in the relation between the roll-rate P and control (aileron) deflections. This transfer function is:

$$\frac{P(s)}{\delta_a(s)}=\frac{b_1s+b_0}{s^2+a_1s+a_0} \tag{2.50}$$

where δ_a is the combined deflection effect of the aileron in radians (positive is down, however ailerons deflect anti-symmetrically).

Here we assume that Φ is small and that forces caused by control surfaces are linear to deflections and body forces are linear to α or β.

Coefficients of a_i and b_i in Eq. (2.50) are the following:

$$a_1=\frac{q\cdot S_{body}\cdot C_{yB}}{u_0\cdot m}-\frac{q\cdot S_{body}\cdot C_{L\beta}\cdot l_{cp}\cdot l}{I_x}$$

$$a_0=\frac{q^2\cdot S_{wing}^2\cdot C_{y\beta}\cdot C_{L\beta}\cdot l_{cp}\cdot l}{u_0\cdot I_x\cdot m}-\frac{q\cdot S_{wing}\cdot C_{L\beta}\cdot l_{cp}\cdot l_{cs}}{u_0\cdot I_x\cdot m}$$

$$b_1=\frac{q\cdot S_{ail}\cdot C_{L\delta}\cdot l_{cs}}{I_x}$$

$$b_0 = \frac{q^2 \cdot S_{body} \cdot S_{ail} \cdot C_{L\beta} \cdot C_{L\delta}}{u_0 \cdot I_x \cdot m} - \frac{q^2 \cdot S_{wing} \cdot S_{ail} \cdot C_{y\beta} \cdot C_{L\delta} \cdot l_{cs}}{u_0 \cdot I_x \cdot m}$$

In case of Sinus 912 motorglider and the set point described in Subsection 2.2 the Eq. (2.50) becomes:

$$\frac{P(s)}{\delta_a(s)} = \frac{0.6075s + 0.2106}{s^2 + 0.4892s + 0.1721} \quad . \tag{2.51}$$

2 IDENTIFICATION OF ACTUAL AIRCRAFT MODEL

Pipistrel Sinus 912 motorglider is the aircraft of choice due to its unique construction, manoeuvrability and performance. One of the challenges when modelling an aircraft in flight is to adequately describe all control interconnection effects and consequent secondary movement effect. On motorgliders, these effects will be more profound, hence making the modelling and identification more challenging.

2.1. Measurements and Identification

In system identification, close attention must be paid to the selection and use of the correct input signals (control movements) as well as to accurate measurements of all the responses. In our case, the input signal is a series of pulses with variable amplitude and frequency to record the aircraft's behaviour as precisely as possible [6]. Of course, pilot skills of the person introducing control movement (pulses) and control mechanism forces limit the frequencies on the higher part of the envelope, while at the lower part the frequency of the control movements is limited with pushing the aircraft into unusual attitudes, e.g. 5 seconds of full aileron deflection will result in inverted flight.

Figure 2 shows the equipment installed in the cabin of the Sinus 912. The logger is in the gray box placed on the seat, exactly in the centre of gravity of the aircraft and the display is there to monitor acquisition of data in flight.

Equipment used to measure aircraft and flight data was the STZAFL 100 Hz data logger, with interface to Matlab. The measured inputs were: aileron movement, elevator movement, rudder movement and engine RPM. Measured outputs were: roll-rate, pitch-rate, yaw-rate, airspeed and altitude. Figure 3 shows input-output relations between aileron deflection and roll-rate as well as elevator deflection and pitch-rate. Superimposed is the identified model (2.52 and 2.53) response. For the data analysis and system identification a 10 Hz sampling rate was used to remove noise.

The system identification performed is a "grey box" parametric approach with the minimisation of square error by calculating the pseudo-inverse of the psi – y matrix. Similar results were obtained also by using Matlab's System identification toolbox.

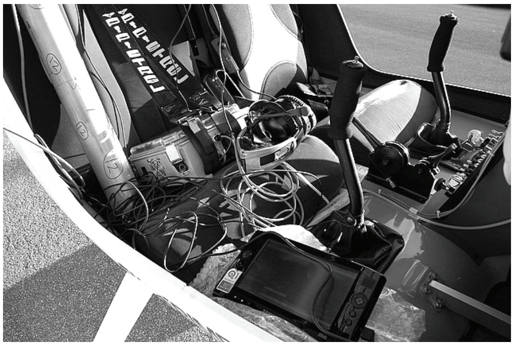

Fig. 2. *Measurement equipment in the cockpit of Sinus 912*

The aircraft is, from the system viewpoint, a highly multivariable structure, however only direct, SISO transfer functions were identified due to a more direct further inter-model performance comparisons.

A second order transfer function was imposed for each of the aileron-to-roll-rate and elevator-to-pitch-rate behaviours, so only parameter estimation was performed. Note that this also offers a more direct comparison between the theoretically derived and identified transfer functions.

The elevator-to-pitch-rate transfer function obtained with system identification is:

$$\frac{Q(s)}{\delta_e(s)} = \frac{7.6230s + 1.5753}{s^2 + 0.3481s + 0.1306} \quad . \tag{3.1}$$

The aileron-to-roll-rate transfer function obtained with system identification is:

$$\frac{P(s)}{\delta_a(s)} = \frac{0.2738s + 0.1880}{s^2 + 0.3785s + 0.1393} \quad . \tag{3.2}$$

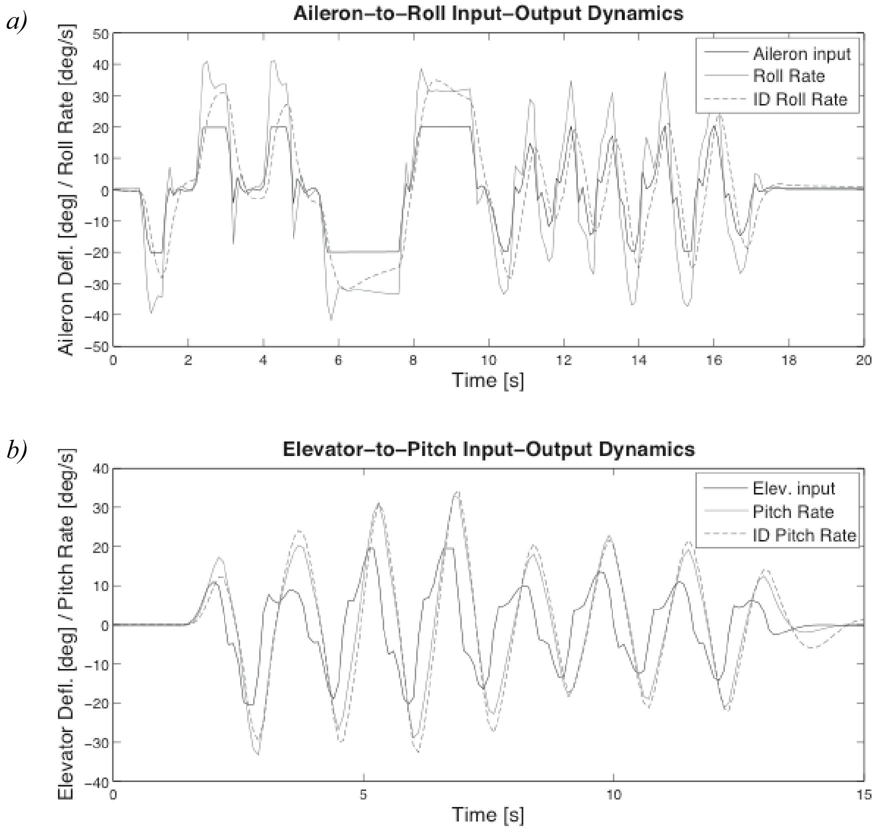

Fig. 3. *Input-Output data used for model identification and the identified solution (ID)*

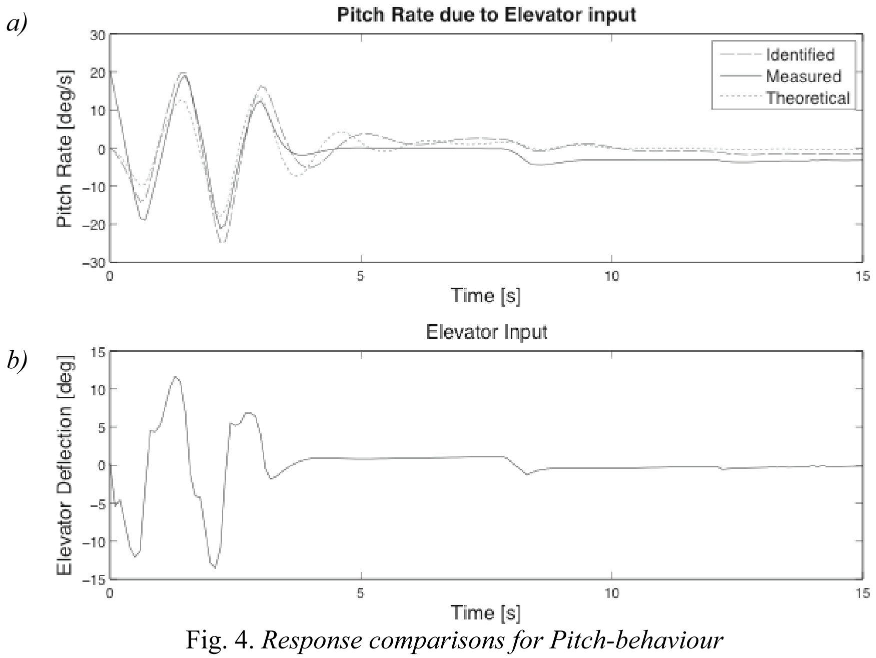

Fig. 4. *Response comparisons for Pitch-behaviour*

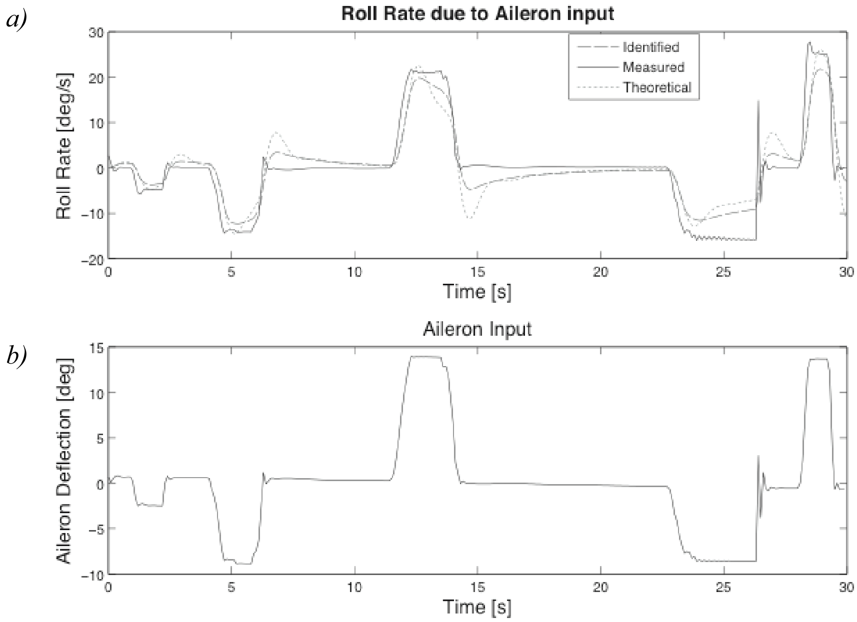

Fig. 5. *Response comparisons for Roll-behaviour*

2.2 Validation and Model Comparison

The validation of the results was carried out by comparing the simulated response against the actual measured response on a set of data which were different from those used for system identification.

For the purpose of model performance comparison between the theoretical and identified aircraft models a Simulink model was developed. It allows simultaneous simulations and output comparisons of the two derived dynamic models. Fig. 4 and 5 show comparisons of measured flight data against the simulated responses of the theoretically obtained transfer functions (2.49) and (2.51). Input is common for all three responses and is the measured input obtained during actual flights.

Fig. 4 shows the responses of the two derived elevator-to-pitch-rate transfer functions against the actual measured response (top chart). The elevator inputs are presented in the bottom chart. While there are differences in amplitudes and overshoots at certain points of the measured elevator inputs, it is evident that both theoretical and identified pitch-behaviour models adequately describe the behaviour of the full-scale aircraft in motion.

Fig. 5 reveals that the differences between the actual aircraft response (dashed line, top chart) and the two derived transfer functions of second order are higher than those in Fig. 4 for the aircraft's pitch behaviour. The mentioned differences in modelling roll behaviour of an aircraft arise due to larger aerodynamic couplings between the wings' fixed and moving structures, which are difficult or impossible to describe accurately. Nevertheless, both the theoretical and identified transfer functions for roll-behaviour adequately describe the aircraft's motion for simulation and control applications.

In essence, three datasets are compared. There is the measured input-output dataset, where the actual behaviour of the aircraft is presented for both elevator and aileron extitations.

The second dataset is the theoretical model reponse, obtained through simulation using data from the real world as the input and the transfer functions (2.49) and (2.51). This dataset shows how well the behaviour of an aircraft, which is determined purely theoretically by means of geometric properties and aerodynamic coefficients, matches the real behaviour of the aircraft – the theory versus practice question.

The second dataset is the identified model reponse, obtained through simulation using data from the real world as the input and the transfer functions (3.1) and (3.2). These transfer functions were obtained using the real-world measurements alone, without taking into account any known data about the aircraft. This dataset shows how well the discussed behaviour of the aircraft can be described with a rather simple second order transfer function (linear model).

3 CONCLUSION

The design phase of an aircraft's development has changed during the years. In an attempt to cut costs various development teams have already decided to eliminate the prototyping phase for aircraft structural evaluations and testing. The fact that the theoretically derived aircraft dynamic model closely matches the identified one indicates that the flight test phase during aircraft development could be reduced to a mere parameter validation. Using theoretical aircraft motion models the designers can, with a great degree of confidence, fly the aircraft in a virtual environment before the actual physical airframe takes flight.

Even though the results may not seem satisfactory at a first glance, it can be concluded that amplitudes, as well as time dynamics of the theoretical model mimic the actual flight performance of the aircraft relatively well. It was shown that the model obtained using combined theoretical-experimental approach, which is most often the situation in practical cases, indeed describes the behaviour of the real aircraft adequately. In certain cases (fast dynamics), it outperforms the identified aircraft model. This is due to the fact that aerodynamic forces rather than just linear input-output dynamic were taken into account.

This paper is focused around a single set-point (420 kg take-off weight, 140 km/h) and the derived theoretical model is linear for simplicity of parameter estimation. Of course such a model cannot be used to mimic the behaviour of the aircraft across the whole operational envelope, as aircraft dynamics normally exhibit large degrees of non-linearity. The purpose of the paper was to show whether a purely theoretical approach can describe the behaviour of a full scale aircraft for a certain set point. Having proven that this can indeed be achieved with adequate precision to also support engineering decisions during the design phase, the same theoretical approach could also be used to assemble a quasi-nonlinear aircraft model, which could be used to simulate the complete operation envelope of the aircraft rather. Such a quasi-nonlinear model would be formed by fuzzy-coupling of a multitude of purely linear theoretical aircraft dynamic models for a number of given and computed set-points spread across the operational envelope. The method of obtaining the theoretical aircraft model is simple enough to be run in real time in Matlab and uses relatively few dimensional parameters, which can all be derived through CAD/CFD analysis. The benefits of testing the aircraft's behaviour in a virtual environment are not only time and cost savings – such an approach also greatly reduces environmental stress, especially when dealing with larger aircraft.

4 ACKNOWLEDGEMENTS

Operation part financed by the European Union, European Social Fund.

5 REFERENCES

[1] Tomazic, T and Matko, D. (2007) Configuration of UAV Autopilots' dynamics using a 3 DOF aircraft motion Simulator, *Proceedings of the 6th EUROSIM Congress on Modelling and Simulation*, Vol 2, Ljubljana, September 2007, p. 1-8.

[2] Guidorzi, R., Diversi, R. and Soverini, U. (2007) Identification Techniques in VNAV Autopilot Design for a Light Sport Aircraft, *Proceedings of the 6th EUROSIM Congress on Modelling and Simulation*, Vol 2, Ljubljana, September 2007, p. 1-6.

[3] Cvetković, D., Radaković, D. (2007) Mathematical Models of Helicopter Flight Dynamics,: *Strojniški vestnik - Journal of Mechanical Engineering, Vol 53, No.* 2, p. 114-126.

[4] Pipistrel d.o.o. Ajdovscina (2006) *Flight manual and Maintenance Manual for Sinus 912 Motorglider.* Retreived on 1.3.2009, z http://www.pipistrel.si

[5] Matko, D., Karba, R. and Zupancic, B. (1992) *Simulation and Modelling of Continuous Systems: A Case Study Approach.* Prentice Hall, Oxford, ISBN 978-0138080648

[6] Stevens, Brian L. and Lewis, Frank L. (2003) *Aircraft Control and Simulation.* Wiley-Interscience. Hoboken, NY, ISBN: 978-0471371458

[7] Tischler, M and Remple, R. (2006) *Aircraft and Rotorcraft System Identification: Engineering Methods With Flight-test Examples.* American Institute of Aeronautics and Astronautics. Reston, VA, ISBN: 978-1563478376